

SAND98-1396C  
SAND-98-1396C  
CONF-980818-

# THE EFFECTS OF ELECTRODE CLEANING AND CONDITIONING ON THE PERFORMANCE OF HIGH-ENERGY, PULSED-POWER DEVICES

M. E. Cuneo

JUN 30 1998

OSTI

Pulsed Power Sciences Center, Sandia National Laboratories,  
Albuquerque, NM 87185-1186 USA (mecuneo@sandia.gov)

**Abstract** - High-energy pulsed-power devices routinely access field strengths above those at which broad-area, cathode-initiated, high-voltage vacuum-breakdown occur ( $> 1e7 - 3e7$  V/m). Examples include magnetically-insulated-transmission-lines and current convolutes, high-current-density electron and ion diodes, high-power microwave devices, and cavities and other structures for electrostatic and RF accelerators. Energy deposited in anode surfaces may exceed anode plasma thermal-desorption creation thresholds on the time-scale of the pulse. Stimulated desorption by electron or photon bombardment can also lead to plasma formation on electrode or insulator surfaces. Device performance is limited above these thresholds, particularly in pulselength and energy, by the formation and expansion of plasmas formed primarily from electrode contaminants. In-situ conditioning techniques to modify and eliminate the contaminants through multiple high-voltage pulses, low base pressures, RF discharge cleaning, heating, surface coatings, and ion- and electron-beam surface treatment allow access to new regimes of performance through control of plasma formation and modification of the plasma properties. Experimental and theoretical progress from a variety of devices and small scale experiments with a variety of treatment methods will be reviewed and recommendations given for future work.

## 1. INTRODUCTION

Large-scale, multi-module, high-energy, pulsed-power devices have been developed world-wide to study the physics of high-energy-density states of matter. Applications include inertial confinement fusion (ICF) with light ions and Z-pinchers, plasma radiation sources, bright bremsstrahlung sources for gamma ray simulators and radiography, and power conditioning systems for large lasers and accelerators. Other, somewhat smaller scale applications such as microwave sources and ion and electron beam surface treatment systems are also being developed.

Pulsed-power technology is based on power compression in several stages by means of a series of fast closing or opening switches where high voltage is developed at metal and insulator surfaces in gases, liquids (oil, water), vacuum, and plasmas. The power-compression, power-transmission and load regions of these devices may routinely require electric fields of more than  $1e7$  to  $3e7$  V/m where broad-area, cathode-plasma-initiated, high voltage breakdown or surface flashover occur under technical vacuum conditions ( $\approx 1e-5$  Torr) without conditioning. Enhanced-field-emission (EFE) leads to cathode heating in local spots by several proposed mechanisms [1-4] and can result in local surface temperatures well above  $1000$  °C, with a specific energy deposition in the range of  $1 - 10$  kJ/g adequate to vaporize a metallic electrode as well as desorb and ionize contaminants. These local processes lead to cathode plasma formation and expansion. High-power densities, particle flux and joule heating in the transmission and load regions can also exceed anode plasma

creation thresholds from contaminants ( $> 50$  J/g depending on material) [5-9] on the time-scale of the pulse.

This paper will examine the role of surface and bulk electrode contamination in anode and cathode plasma formation in pulsed-power devices, discuss cleaning and conditioning techniques which are possible for the mitigation of anode and cathode plasmas, and review experiments on contaminant effects, conditioning and cleaning in a variety of small scale experiments and large pulsed-power facilities.

## 2. ELECTRODE PLASMAS

Anode and cathode plasmas cause many undesirable effects in pulsed power devices and have been the subject of considerable study for decades [10-15]. Although in many applications cathode and anode plasmas in vacuum gaps are a desirable (and inescapable) aspect of device operation, these plasmas ultimately limit the system scalability and performance. Vacuum gaps with plasmas are actually in the process of breakdown. The load must perform its function in the period prior to gap shorting. Anode-cathode (AK) gap plasma closure leads to impedance collapse, limitations on the pulse length and total energy that can be delivered to a load, and many other application specific effects discussed below. Device design requires careful attention to electric fields and particle flux to minimize the creation of these plasmas. Elimination or modification of these plasmas would significantly improve performance in many applications.

Spectroscopic studies of the composition of anode and cathode plasmas in vacuum gaps of high-power devices show a dominant inventory consistent with formation from hydrocarbon surface and bulk contaminant layers or the heating and breakdown of dielectric inclusions. Emission and absorption lines of C, and O, as well as neutral H are observed [6,9-11,14,15]. Cathode plasma gap closure rates are thought to be dominated by hydrogen [10]. Although metallic lines from electrode material are observed, they are not dominant with a broad-area geometry as they appear to be with needle cathodes [16]. Protons and multiple charge states of C and O (and other anode electrode materials) are observed in particle-sensing diagnostics such as Faraday cups, Thomson parabolas, and magnetic spectrometers. [6,8,17,18].

### 2.1 Contaminant Inventory

We concentrate on the role of adsorbed contaminant and oxide layers, although dust particulate [19] and dielectric- or insulated-metallic inclusions [1] also affect breakdown and flashover and can be modified by conditioning techniques. Typical base vacuum conditions for large-scale systems are on the order of  $1$  to  $5e-5$  Torr. The cleanliness of the operating environment and the vacuum conditions are dominated by the size of the device, shot-rate requirements with vacuum opening once to a few times per day, and the destructive nature of a single-shot event which liberates and spreads contamination. RGA (Residual Gas Analysis) of

## **DISCLAIMER**

This report was prepared as an account of work sponsored by an agency of the United States Government. Neither the United States Government nor any agency thereof, nor any of their employees, makes any warranty, express or implied, or assumes any legal liability or responsibility for the accuracy, completeness, or usefulness of any information, apparatus, product, or process disclosed, or represents that its use would not infringe privately owned rights. Reference herein to any specific commercial product, process, or service by trade name, trademark, manufacturer, or otherwise does not necessarily constitute or imply its endorsement, recommendation, or favoring by the United States Government or any agency thereof. The views and opinions of authors expressed herein do not necessarily state or reflect those of the United States Government or any agency thereof.

vacuum systems show partial pressures dominated by four main gases: H<sub>2</sub>, H<sub>2</sub>O, CO, CO<sub>2</sub>. Under these conditions, on the order of 100-300 Å (30 - 100 monolayers (ml), each ml ≈ 1e15 particles/cm<sup>2</sup>) of porous surface oxides (e.g. on aluminum or stainless) are present which contain these gases (and others, e.g. hydrocarbons, C<sub>n</sub>H<sub>m</sub>) on the surface and in the bulk of the oxide [20-22]. Note that a significant fraction of this inventory contains hydrogen. These four primary contaminants show binding energies on relevant electrode materials in the range of 10 - 40 kcal/mole (0.43 - 1.74 eV) [20-30]. Surface oxides which are present are more tightly bound (> 50 to 90 kcal/mole).

The surface inventory is determined by desorption and readsorption rates [19,23,24]:

$$\frac{dn}{dt} = -v_x n^x \exp\left[-\frac{Q}{RT}\right] + \frac{3.5e22sP}{\sqrt{MT}} \left(1 - \frac{n}{n_a}\right)^x \quad (1)$$

where the first term describes thermal desorption of contaminants and the second readsorption resulting from background gas collisions with the surface. In this equation,  $dn/dt$  is the desorbed flux in atoms/cm<sup>2</sup>/s,  $n(t)$  is the instantaneous surface coverage in atoms/cm<sup>2</sup>,  $v_x$  is the rate constant for the desorption ( $v \approx 10^{13} \pm 1$  s<sup>-1</sup> for  $x=1$ , first order,  $\approx 10^{-4}$  to  $10^{-1}$  cm<sup>2</sup> s<sup>-1</sup> for  $x=2$ , second order),  $Q$  is the binding energy for the contaminant (kcal/mole),  $R$  is 1.9858e-3 kcal/mole/K,  $T$  is the gas and electrode temperature in °K,  $s$  is the sticking coefficient,  $P$  the gas pressure in Torr,  $M$  the gas atomic weight in amu, and  $n_a$  is the number of sites available for adsorption. Eq. 1 is only approximately correct for adsorption of the first monolayer, since we assume  $s=1$ , and sufficient adsorption sites to get a maximum rate of readsorption.

In order that desorption rates exceed the maximum recontamination rate from the background gas in Eq. 1 by a factor of 10, at 1e-5 Torr and  $n=0.1$  ml, we require  $T/Q \approx 21.7$ . At room temperature (293 °K), we find that surface contaminants are depleted below  $Q \approx 13.5$  kcal/mole. Efficient removal of water vapor and various hydrocarbons from the chamber walls and surface oxide layers with binding energies of 20 to 40 kcal/mole (at  $T/Q > 21.7$ ) requires extended periods at  $T > 160$  to 600 °C for depletion. These arguments explain why vacuum system pump down times at room temperature appear to be limited by contaminants with intermediate binding energies in the range of 14 to 50 kcal/mole [26]. At higher binding energies the desorption rates at room temperature are so small that the system vacuum is not influenced, although this tightly bound inventory can still be desorbed in experiments under the correct conditions.

## 2.2 Pulsed Desorption from Electrodes

The scaling of desorption from a contaminated electrode surface can be examined with [18,22]:

$$\frac{dn}{dt} = -v_x n(t)^x \exp\left[-\frac{Q}{RT(t)}\right] \frac{J_p(t)\sigma n(t)}{e} \quad (2)$$

where the first term describes thermal desorption of contaminants as above and the second, stimulated desorption. Readsorption from the background gas, considered above, is negligible because of the rapid time scale of the desorption during the power pulse. In this

equation,  $T(t)$  is now the instantaneous electrode surface temperature,  $J_p(t)$  is the instantaneous particle current density (primary and secondary, electrons or ions),  $\sigma$  is the cross-section for stimulated desorption, and  $e$  is the unit charge.

Power deposition in anode surfaces by: (i) primary or secondary electrons, (ii) negative ions [31], or (iii) joule or resistive heating at high current flow [32], can heat up the anode surface to temperatures  $\geq 1000$  °C on the timescale of the pulse. Under these conditions, stimulated desorption rates are negligible compared to thermal desorption rates [18,33] because cross sections are small at MeV electron energies. Thermal desorption exceeds stimulated desorption by a factor of 10 at  $J_e=1$  kA/cm<sup>2</sup>,  $\sigma=1e-17$  cm<sup>2</sup> (1e-15 cm<sup>2</sup>) when  $T/Q > 30$  (42), or  $\approx 150$  °C (310 °C) at  $Q=14$  kcal/mole. Hence for low temperatures and high particle flux, stimulated desorption is important. Halbritter [34] has emphasized the role of stimulated desorption of contaminants at limiting the breakdown and flashover strengths to the 1e7 V/m range. Stimulated desorption is important in (i) the initiation of events on anode and cathode surfaces at low temperature, (ii) under special conditions with high current densities or avalanches of low energy ( $\approx 1$ -100 eV) electrons, and (iii) with particular contaminants with high elastic scattering cross section [34]. Stimulated desorption possibly accounts for temperature independent anode particle production early in the power pulse in several works [8,18,35], may be a dominant effect in insulator flashover [36,37], in cavities for RF accelerators [19,38], and in microwave devices.

Neglecting stimulated desorption, Eq. (2) is solved formally for  $F$ , the fraction of contaminants on the surface that have been thermally-desorbed (first order,  $x=1$ ):

$$F = 1 - \frac{n(t)}{n_0} = 1 - \exp\left[-v \int \exp\left(-\frac{Q}{RT(t)}\right) dt\right] \quad (3)$$

where  $n_0$  is the initial inventory. The double exponential dependence implies that for experiments where temperature rises quickly, this function is approximately a desorption step function at a fixed time. Complete desorption ( $F=1$ ) of a particular  $Q$  is approached within 10-15 ns for rapid anode heating rates [18]. As  $Q$  increases, the critical time for desorption moves later, to higher temperature.

Significant thermal desorption of 1 to 10 ml in pulsed experiments on a 10 ns to 500 ns timescale requires desorption rates  $v \exp(-Q/RT) \approx 10^6$  to  $10^9$  s<sup>-1</sup>. This implies  $T/Q > 32.4$  to 54.3 or  $T \approx 180$  to 490 °C for  $Q = 14$  kcal/mole. This temperature range bounds those where anode plasma effects have been observed. Anode plasmas are observed at surface temperatures estimated to be in the range of 250 to 600 °C in a wide variety of experiments [5-9], and are much lower than those for cathode or anode spot formation. Anode plasma production is proportional to the specific heat of the anode material [6-8], indicating a thermal desorption mechanism. Anode plasma formation required a surface temperature of  $400 \pm 60$  °C independent of three materials studied [8]. As noted above, these temperatures are typically used to clean metal surfaces and bulk in vacuum baking.

The relationship between binding energy  $Q$  and  $T_p$ , the temperature at the peak in the thermal desorption rate  $dn/dt$  satisfies [39,40]:

$$\frac{Q}{RT_p^2} = \frac{v \exp(-Q/RT_p)}{dT/dt} \quad (4)$$

63% of the inventory for a first order system has already desorbed when the peak desorption rate is reached, so this is a good estimate of the temperature at which contaminant desorption will dominate. Eq. 4 was solved for the ratio  $Q/T_p$  with a linear temperature history  $T(t) = T_0 + at$ , with  $v = 1e13$ . Heating rates (governed by a) typical of pulsed-power experiments were chosen to give  $\Delta T = T - T_0 = 500$  °K in 10 to 500 ns timescales. The results of  $T_p$  vs. time for  $Q = 14$  and 17 kcal/mole are plotted in Fig. 1. The upper and lower bound temperatures and pulselength at which ion or anode plasma effects are observed are averaged and plotted (triangles) from 4 short pulse experiments [5-8]. This data agrees with the predictions of Fig. 4 for the temperatures at which the peak desorption rates occur. Anode plasma effects will be observed at lower temperatures for longer pulselengths since the desorption rate peaks at a lower temperature. This also agrees with experimental data (circles) where ion effects appeared on a 500 ns timescale [9]. These arguments link anode plasma formation with thermal desorption of the readily available contaminant inventory with  $Q > 14$  kcal/mole.

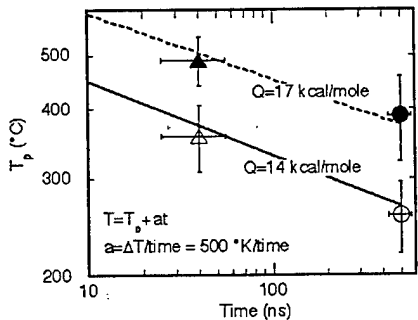


Fig. 1. Temperature at peak desorption rate for a linear temperature history, and different heating rates compared with experiments [5-9].

Processes on the cathode such as: (i) metallic-whisker heating and explosion [1], (ii) “dielectric-assisted” hot electron emission leading to dielectric heating and destruction [2], (iii) cathode spot migration [41], (iv) ion bombardment [42], (v) joule or ohmic heating at high current flow [32,42] and others, each would also lead to thermal and stimulated desorption. Although the heating rates are larger than for the anode, there is larger uncertainty about spot sizes, and heating mechanism. Still, the contaminant vapor density exceeds that for metals and their oxides by many orders of magnitude up through perhaps temperatures where contaminants have been depleted (above the oxide or material melting temperatures). For example, the vapor pressure for Cu at 1530 °K is 1e-02 Torr, at which the Cu particle flux leaving the surface is about 1e3 ml/s. Surface contaminant thermal desorption rates at  $Q=20$  kcal/mole are more than 1e6 ml/s at about 620 °K. Although contaminant plasmas may not be able to sustain the cathode spot ignition and migration processes, and cannot supply the flux for steady arc operation on a longer timescale, they are desorbed earlier, expand faster, and are easily ionized, dominating the expanding, field-excluding, plasma boundary in short-pulsed experiments.

We must be cautious applying Eq. 2 to the desorption of the entire ≈ 100 ml inventory of contaminants on the surface and

in the oxide layer. Although desorption and ionization of contaminants is the dominant source of anode and cathode plasmas based on the large effects of contaminant cleaning discussed below, the rate-limiting steps for neutral desorption can be dominated by processes other than surface desorption such as surface migration and recombination, and bulk, oxide and defect-assisted diffusion. These processes are sensitively dependent on the properties of the oxide layer [43]. This is a subject for ongoing research.

A complete treatment of the ionization of these neutral layers is beyond the scope of this review. The neutral layer front expands at about 3 times the gas sound speed into vacuum [44,18], e.g. velocities of > 6 μm/ns are expected for H<sub>2</sub> neutrals at > 400 °C. A layer thickness (vt) of 60 μm is therefore reached in 10 ns (without additional heating). Rapid desorption (Eq. 3) of 1 to 10 ml produces average densities in the expanding neutral layers ≈ 1e23-1e24 m<sup>-3</sup> [44]. At these densities, only modest ionization rates are required to produce ≈ 1e19 m<sup>-3</sup> electron and ion densities in 10 ns, which are sufficient to begin screening the AK gap electric field and to supply ions and electrons to the gap. Secondary electron or ion avalanches and complete ionization are possible with layers of 100 to 500 μm thick depending on the magnitude of E and B in the neutral layer. Hybrid PIC-fluid codes are required to determine the effect of neutral desorption, ionization, plasma heating and expansion, and charge-exchange processes on high-voltage gap behavior [45,46]. These tools have been applied to the modeling of LiF field-threshold ion source shut-off [45,18].

### 3. CLEANING AND CONDITIONING TECHNIQUES

The influence of dielectrics and contaminants is observed in DC and pulsed high-voltage gap electron emission and breakdown studies. There is a large body of work that shows a significant role for dielectric-thin-film layers (oxides or contaminants), dielectric inclusions, and metallic and non-metallic particulate matter in initiating, mediating and modifying electron emission from electrically-stressed metal surfaces in vacuum [1,2,4,47]. Adsorbed gas can change the work function for metallic emitters, and cause large fluctuations in pre-breakdown electron emission [2]. Particulate may largely determine breakdown voltages, at least for DC experiments [48]. Carbon particulate is particularly emissive.

Conditioning techniques for high-voltage gaps include [4,47-51]: (i) extensive in-situ heating for up to 10's of hours to 250 to 1800 °C at low base pressures < 1e-8 Torr [48-51], (ii) discharges [49,50,52], (iii) pre-breakdown electron emission or gas conditioning [47,49-51], and (iv) conditioning with multiple breakdowns or arcs. The latter are the most effective [47,50]. Pulsed and DC electric fields of up to 5e7 to 1.4e8 V/m [1, 47-51] have been possible with these techniques, compared to 1e7 to 3e7 V/m without them [34], by reduction of surface gases, and conditioning or elimination of particulate prebreakdown electron emission sites. Other techniques which have been used are: (v) surface coatings [53-55], (vi) ion implantation [56], and (vii) multiple pulse electron beam irradiation [57]. These last techniques all appear to give about a factor of 2 increase in voltage holdoff. Extensive pre-installation conditioning of superconducting Nb cavities also utilize chemical etching, or electropolishing to remove particulate, and water rinsing and clean room assembly techniques to eliminate dust [38,58].

Several of the most effective techniques that are used in small-scale breakdown experiments e.g. (iii) and (iv) above, are difficult or impossible in large-scale pulsed-power environments. Electric field levels in pulsed power systems are in the range of  $10^8$  to  $10^9$  V/m in the vacuum gaps of transmission lines and diodes, which exceeds breakdown thresholds for unconditioned electrodes by more than a factor of 4 - 10. Unless complete suppression of EFE and plasma formation is accomplished, a factor of 2 improvement in breakdown voltage is of limited application. An improvement of breakdown fields routinely to  $10^8$  V/m would be beneficial in many applications. As noted above, the conditions in pulsed-power experiments have limited base pressures to the 1 to  $5 \times 10^{-5}$  Torr level. High-energy experiments are inherently single-shot, although some experiments at lower-power have been able to use multiple-pulse conditioning. Treatment methods which may be reasonable for electrode areas of  $> 1 \text{ cm}^2$  become difficult at  $> 10 \text{ m}^2$ , particularly when the surfaces become unconditioned after a single event and at least one shot per day is required. Of the in-situ techniques considered above, improvement of voltage holdoff in pulsed-power systems may be limited to heating or discharges for large-area, high-energy systems. Other pre-installation conditioning techniques, e.g. electron [57] or ion beam surface treatments should be developed. Multiple-pulse electron beam irradiation and melting with  $1 - 5 \text{ J/cm}^2/\text{pulse}$  has shown a factor of 1.5 to 2 increase in gap voltage holdoff for  $\approx 1 \text{ cm}^2$  size samples [57] possibly from surface hardening, smoothing, and cleaning.

The goal behind cleaning when electrodes are exposed to fields and power densities where breakdown is unavoidable, is to beneficially alter the properties of the plasmas that are formed. Control of the surface and bulk contamination that dominate plasma composition could lead to a breakdown or plasma formation delay, a change in composition, and an increase in the effective mass of the plasma (by control of hydrogen) and thus a decrease in its expansion velocity [10]. The plasma density, and uniformity may also be modified. Several of these effects may be responsible for observations in experiments with cleaning. The application of multiple pre-installation and in-situ techniques in parallel or sequence has been found to be important in pulsed power [18] as has been observed in the conditioning of superconducting Nb cavities for high-energy electron beam acceleration [38,58]. Performance improvements have followed routinely as the thoroughness of cleaning and conditioning has increased.

Heating to 100 to 1000 °C has been the most common technique applied in the pulsed-power field. DC and pulsed heating techniques (ohmic, inductive, or laser-driven) have been developed. Pulsed heating techniques largely aim to deplete surface layers or quickly melt oxides (surface and oxide control) at large temperatures, without the added difficulty of cooling for other subsystems, e.g. field coils for ion diodes. DC heating techniques are more appropriate to deplete bulk oxide layers of water vapor and hydrocarbons with long bakeouts. Creation or precipitation of carbon during heating should be avoided.

Small-scale experiments have shown that thermal activation or impurity migration can lead to an increase of the number of particulate pre-breakdown emission sites on cathodes up through a peak at about 800 °C on Nb [48]. The strength of emission sites is also increased by heating up through 400 °C [2]. Breakdown strengths are correlated to both the

number and strength of emission sites. Elimination of emission sites and an increase in breakdown voltage on Nb required heating  $> 1400$  °C [48], temperatures which have not yet been applied to conditioning for pulsed-power systems. The decrease of emission with higher temperatures cannot be arbitrarily applied to materials. Heating to 650 °C (and Ar ion sputtering) was unable to mitigate EFE from Al cathodes [59]. EFE from Al cathodes was very robust.

Surface coatings have been used to control desorption from both cathodes and anodes and to provide a cleanable seal, with varying degrees of success. Material chemisorption properties are important [24,25] in the selection of the film; Au films have minimal chemisorption. There are important differences in film purity (and morphology and surface coverage) depending on deposition technique varying from electroplated films with high impurity and particulate content to sputtered and evaporated films with lower contamination. Coatings have been also used to increase the breakdown threshold [55], and increase surface flashover strength.

Surface heating cannot clean the oxide layers off of materials without very high temperatures that could be impractical in real devices [48, 60]. DC and RF discharges have proven to be efficient at physical and chemical sputtering of even the most resistant surface oxides at temperatures that are realistic. Particle fluxes of roughly  $2 \times 10^{18}$  ions/cm<sup>2</sup> have been shown to generate an atomically cleaned surface free of C on stainless with Ar/O<sub>2</sub> discharges [61,62]. Larger fluxes of  $> 2 \times 10^{19}$

ions/cm<sup>2</sup> are required when using Ar physical sputtering without O<sub>2</sub> [61,62]. The combination of heating and discharges allows a further increase in impurity removal rate. Oxygen in discharges remove hydrocarbons from surfaces at a higher rate than pure physical sputtering by converting them to H<sub>2</sub>O, CO, and CO<sub>2</sub> for a higher effective removal rate. Pulsed-power applications want to minimize hydrogen, hence Ar and Ar/O<sub>2</sub> mixtures are used to maximize the mass. There are several factors ensuring that the discharge actually removes contaminants from the vacuum chamber, i. e. it is a "cleaning discharge". For a more complete description of many issues important in discharge cleaning refer to [18,20,21,52,61-64]. Reactive discharges have proven very effective at conditioning high-voltage systems [52], and altering field emission [65] and secondary electron emission properties [66], proving indirectly the important role the electrode surface state has on device operation.

Measurement techniques such as XPS (X-ray Photoelectron Spectroscopy), AES (Auger Electron Spectroscopy), SIMS (Secondary Ion Mass Spectroscopy), and TPD (Temperature Programmed Desorption) are useful for characterizing the pre- and post-cleaning contaminant inventory with varying degrees of quantitative precision [25,30,39,40]. For example, the efficacy of various discharge cleaning protocols for LiF ion source films for ICF has been measured with XPS [64]. These studies indicated that 15 minutes of an Ar/O<sub>2</sub> discharge ( $1$  to  $3 \times 10^{17}$  ions/cm<sup>2</sup> sputtering flux) was sufficient to reduce an initial 13 - 45 monolayers of carbon impurities in the first 200 Å of the LiF surface to  $\leq 2 - 4$  monolayers, replicating the original, as-coated condition.

The efficacy of discharge cleaning has also been measured with TPD. Fig. 2 shows that the thermal desorption of H<sub>2</sub> neutrals from unconditioned stainless through about 450 °C is reduced by a factor of 10 with discharge cleaning in Ar/O<sub>2</sub> from about 5 to  $< 0.5$  ml (calibrated within  $\pm 20\%$ ). These

data were taken with a 9 minute delay following discharge cleaning. These measurements also indicate a factor of about 4 reduction in H<sub>2</sub>O (from 40 ml to 10 ml - uncalibrated) and a factor of 7 reduction in CO with cleaning. CO<sub>2</sub> desorption has not been affected with Ar/O<sub>2</sub> cleaning, an important area for further work. These results show that quantity of desorbed material is decreased and the average mass of the desorbates has been reduced, primarily through reduction of H<sub>2</sub>. Related work showed that Ar/O<sub>2</sub> cleaning reduced the outgassing of metals in vacuum through the formation of a thick oxide layer in vacuum [67].

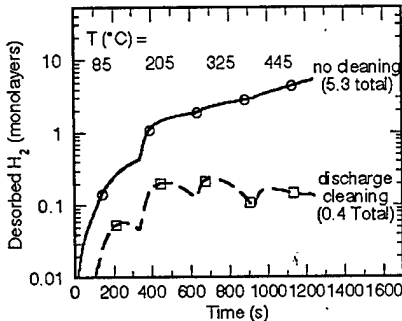


Fig. 2. TPD results for H<sub>2</sub> inventory before and after Ar/O<sub>2</sub> discharge cleaning of stainless steel electrode materials.

#### 4. CLEANING AND CONDITIONING IN PULSED POWER DEVICES

In this section we will review the work that has been done on cleaning and conditioning in a variety of pulsed-power devices. Techniques considered below are in-situ heating, discharge cleaning, surface coatings, and cryogenic cathodes. Material selection has also been important. Conditioning effects have been observed in several low-power experiments. In each section anode plasma mitigation is discussed first, followed by cathode plasma mitigation.

##### 4.1 Magnetically Insulated Transmission Lines (MITL's) and current convolutes

Magnetically-Insulated-Transmission-Lines (MITL's) are a critical element of power transmission, addition, and compression in high-energy, pulsed-power systems. Application to ICF requires transmission of power densities  $\gg 1 \text{ TW/cm}^2$  to the load region. These power densities generate  $\gg 2e7 \text{ V/m}$  fields on aluminum and stainless electrode surfaces [68]. Cathode plasma and electron emission have been observed at these fields [14,68,69]. Pulsed-power systems rely on the self-magnetic field of large current flow in the MITL to prevent the loss of electron current [68]. These devices can be quite efficient at transmitting current and energy to the load. Current and power transmission efficiencies of 60 to 90% can be achieved depending on the load impedance, and system configuration. Even though these devices are efficient, there are gains possible by suppressing cathode plasma formation and electron emission. A factor of 4 improvement in the threshold field from  $2.5e7$  to  $1e8 \text{ V/m}$  would result in significant power gains for some systems, suppressing the insulated-wave [69], possibly enabling higher voltage, smaller AK gaps, and higher current transfer efficiency through current convolutes used for current addition to drive Z-pinches [70]. Further work should be done to increase the electric field thresholds over large areas [57].

Limited work has been done on the effects of cleaning on MITL power flow. Plasma discharge cleaning with reactive gases has increased the operating impedance of the MITL near the ion diode on the PBFA-X experiments described below in section 4.3, by of order 20% [18]. 3  $\mu\text{m}$ -thick sputter-coated Au films are used on the MITL and convolute surfaces on the power flow and Z-pinch load areas of the 20 MA Z driver at Sandia [70], as an outgrowth of the Au coatings used for ion sources (discussed in section 4.3 below). When combined with an extensive pre-installation surface polishing, hydrogen firing and baking procedure, this appears to allow smaller anode-cathode gaps without closure than were possible on the Saturn accelerator. Magnetic fields appear to help maintain vacuum insulation in the 2 - 5 mm AK gaps by plasma confinement at  $B > 50 \text{ T}$  [70].

#### 4.2 Electron Diodes

Electron beams have many high-power applications such as the generation of x-rays, microwaves, and high-power densities through pinching. Plasma formation on the surface of the cathode is desired to provide a zero work function emitter that will provide the required space-charge-limited current densities. Expansion of cathode plasma into vacuum at velocities of 1 - 4 cm/ $\mu\text{sec}$  have been spectroscopically observed or inferred from voltage and current data. These velocities are relatively insensitive to conditions with similar results measured in a wide range of devices and timescales [1,3,10,71]. This is not surprising since: (i) the dominant plasma composition is similar, (ii) the conditions and electric fields under which the plasmas form is similar, and (iii) plasma expansion in many applications is adiabatic [1]. Hydrogen is believed to dominate the closure rate of the plasma [10]. Elimination of hydrogen may not appreciably slow the plasma because of non-thermal (supersonic) expansion of other ions [10].

Super-pinched electron beam diodes reaching current densities of up to  $1 \text{ MA/cm}^2$  in spot sizes of order 1 cm require the formation of anode plasma. Ion space charge neutralizes the radial space-charge electric field allowing strong  $v_z B_\theta$  self-field pinching force on the electron orbits. Although ion space charge and anode plasma formation are required, the diode impedance lifetime was limited by plasma shorting. The anodes of electron diodes were heated to 250 to 1000 °C for periods of 5 minutes to 1.5 hours, reducing the impedance collapse rates [72-74]. Although hydrogen ions were effectively reduced, control of carbon contaminants from the bulk of the Ta anode was still an issue even at 1000 °C for 30 min. in [73]. It is likely that not enough time was allowed to completely outgass the anode in-situ. Most surface contaminants are eliminated by temperatures of 1000 °C for 10's of minutes, but outgassing of the huge quantity of gas in the bulk of refractory metals can require temperatures in excess of the oxide melting temperature ( $\approx 2000 \text{ }^\circ\text{C}$ ) for many hours [23].

Control of anode desorption by Au coating was attempted (unknown deposition technique) in an electron beam diode in poor vacuum (1e-4 Torr) [6]. Discharges (unknown protocol) were also applied. No change in the ion onset time was observed. Heating or discharges were not applied simultaneously with coatings. Thick ( $>$  thermal diffusion time) surface coatings were used to show that pinching rates in electron beam diodes depended in a local way on the rate of increase in surface temperature of the anode [7]. Pinching associated with anode ion production could be slowed by

using higher specific heat anode material that slowed the anode temperature rise.

Total gas evolution per pulse from various electron or ion diodes was reduced by a factor of 2 to 3 with a series of closely spaced pulses, where the delay time in between pulses was  $< 1$  min [75]. The length of exposure to ambient conditions, time under vacuum, multiple-pulse conditioning (up to 20 pulses in a series), and bulk cleanliness of anode materials affected the impedance collapse of a long-pulse electron beam diode by altering the anode plasma formation [9]. Cathode plasma conditioning and reduction of closure was noted after 4 sequential shots [76].

Bremstrahlung diodes are being developed driven by the Decade inductive storage technology. Operation of the upstream plasma opening switch (POS) and the required radiation dose output places restrictions on the AK gap and resulting anode loading. Ar and Ar/O<sub>2</sub> discharge cleaning of the AK gap proved to be essential to increase the x-ray energy output, enabling this device to meet its performance milestones [77]. Reactive discharges gave a 40% increase in dose and a 25% increase in x-ray FWHM over nonreactive discharges. It is believed that plasma cleaning mitigated anode plasma formation from the Ta anode, reducing the energy loss into ions.

Modification of cathode plasma closure rates were attempted with in-situ DC heating of Au-coated (unknown heating time and Au deposition technique) Al cathode to 700 °C in an electron beam diode in poor vacuum (1e-4 Torr). Little change in the impedance collapse rate was observed during the first 50 ns of the pulse. H spectroscopic emission lines were reduced by a factor of  $> 10$  while a CII emission line was unchanged. The impedance collapse rate was slowed later in the pulse, but this was believed to result from radiant heating of the anode and suppression of anode plasma formation. The increase in the number and emissivity of emission sites with heating [2,48] or the robust nature of EFE on Al [59], or possibly spurious contamination of the Au films could have been a factor in the null result [10].

In recent work, Ar/O<sub>2</sub> RF discharge cleaning has been applied [78] to a 500 ns pulselength electron beam diode at macroscopic fields of  $< 2e7$  V/m. Electron emission and hydrogen and aluminum spectroscopic emission lines from an Al cathode were completely suppressed for up to 3 minutes following cleaning. Some suppression of current and emission lines was seen out to 9 minutes from the end of the cleaning protocol. Pure aluminum oxide layers generated in-situ are contamination resistant like Au. This turn-off effect is consistent with other work using reactive discharges [52]. The large magnitude of the effect of cleaning here may result from fields near threshold.

#### 4.3 Ion Diodes

Ion diodes use either self- or applied- magnetic fields or electrostatic reflexing to increase the electron residence time in the AK gap and maximize the ion extraction efficiency compared to electrons. Many different geometries are possible. The most efficient geometry has been the applied-B ion diode. Applied-B ion diodes inhibit electron conduction across the anode-cathode (AK) gap with pulsed magnetic fields of 2 to 5 Tesla applied perpendicular to the accelerating electric fields of 1e8 to 1e9 V/m. Electrons drift in the E X B direction, forming a virtual cathode electron sheath. Fluctuations from instabilities drive cross-field transport of the electron sheath, and the sheath responds to ion current by

diamagnetically compressing towards the anode to smaller effective AK gaps [79] allowing larger electric fields. Electron leakage across the magnetic field and these large electric fields can lead to ion beam generation either through stimulated or thermal desorption and ionization of anode contaminants, flashover production of plasma or a field-threshold-emission process. Large ion current density enhancements over those for the original gap space-charge-limited current are possible. This device has shown promise for ICF with light ion beams [80].

Lithium current densities of 1 to 2 kA/cm<sup>2</sup> at 30 MeV are required to scale to fusion conditions. These lithium current densities can only be achieved at electric fields of 5e8 to 1e9 V/m in 1-3 cm AK gaps. The effect of anode and cathode motion on impedance collapse is enhanced relative to electron diodes, as plasmas cross the magnetic field, since the diode voltage is proportional to magnetic field [79]. Anode and cathode plasma generation and expansion must be controlled to permit ion beam generation for the required pulse width of at least 30 ns. In addition to impedance collapse, production of non-lithium contaminant ions dominate the purity of the lithium beam. The effort to generate a pre-formed, pure lithium anode plasma source for ion fusion has, in-part been dominated by the inevitable surface oxides that form when loading lithium-bearing films. A single ionized monolayer can supply the entire beam inventory, hence control of contaminants is critical.

Contaminant control for the production of lithium anode plasmas for light ion beams was first considered in [81]. A pulsed desorption technique was developed for partial control of the surface oxide layer on LiAg films. A 10 ms current pulse ohmically heated a 3 μm thick LiAg film above the LiAg melting temperature ( $\approx 550$  °C). This technique desorbed hydrogen from the LiOH surface layer via a liquid phase reaction in which LiOH was dissolved in the melted LiAg layer. Several 10 ms pulses were required to achieve a 2 order of magnitude reduction in the total pressure burst from small area (10 cm<sup>2</sup>) coupons. Control of the remaining Li<sub>2</sub>O layer would have required heating to 2000 °C.

Lower temperature DC bakeouts (100 - 250 °C) have subsequently been extensively used to control the weakly bound adsorbates on lithium bearing ion source films for flashover-, laser-, or ohmically-produced ion sources. Heating through 250 °C for up to 1 hour was used to desorb water vapor from LiCl flashover ion source [82]. When DC heating was followed by 5 minutes of Ar discharge cleaning, proton beam contamination was reduced to  $< 10\%$ . It was noted that re-sticking on an anode at elevated temperatures must be reduced to account for the persistence of improvement in the beam purity despite poor vacuum and delays of up to 5 minutes before accelerator firing to pump out the discharge gas.

Heating to 120 to 160 °C for 1 to 5 hours made a large difference in impedance collapse and beam inventory for a laser produced anode plasma source on PBFA-II [83]. Without heating, a low impedance was observed and the beam was dominated by hydrogen ions. With heating the late-time diode impedance was improved, and lithium ions appeared. Heating reduced plasma C spectroscopic emission lines by a factor of 3 to 5 and H lines by a factor of 40 [84]. Contaminants were still observed in the beam however, likely from more tightly-bound contaminants and oxides present that require much higher temperatures for removal. The positive effect of low-temperature heating could only

have been from a diffusive desorption of water vapor from the oxide layer consistent with the spectroscopic results. The anode temperature was still elevated at shot time, hence increased desorption (Eq. 1) prevented water readorption in a vacuum environment that was 80% water vapor (5e-5 Torr).

Discharge cleaning [85,86], heating [85], VUV illumination [86] and in-situ deposition [86] were attempted to clean several candidate films for flashover ion sources for ICF. Contaminant ions contributed as much as 30% of the beam in a proton flashover source and 70% of the extracted ion beam current in an LiF flashover ion source [86]. The above techniques resulted in a factor of 2 or 3 increase in the extracted lithium quantity, but a reduction in the absolute magnitude of the ion current. Discharge cleaning in experiments with ohmically-produced lithium sources gave similar results: improved purity, but reduced ion current density [87]. The role of surface contaminants in flashover ion sources were also shown in [88]. Exposure to ambient conditions, multiple pulse beam conditioning and anode material specific heat modified the beam composition.

Discharge cleaning was used in several experiments discussed above, to improve the purity of lithium anode plasmas. These experiments each had some limitations that reduced the discharge effectiveness. High pressure (100 mTorr), DC discharges in non-reactive gases [82,87] had reduced contaminant removal rate, and only cleaned the anode surfaces. RF discharges in reactive gases at low pressure (6-10 mT) had higher removal rate in [85,86], but the RF electrode was outside of the anode and cathode gap of the diode, hence direct sputtering action on the anode and cathode could not occur. 2 min to 5 min firing delays at pressures  $>5e-5$  Torr were used in these experiments to remove the discharge gas from the accelerator prior to firing. These experiments showed several beneficial effects of discharges by modification of anode plasmas: higher diode impedances and reduced beam contamination were observed at the price of reduced total ion current.

An extensive series of experiments on cleaning for ion diodes were described in [17,18]. Four impurity control techniques were applied to a high-power extraction ion diode on the 1 TW SABRE accelerator. Anode heating, sputter-deposited surface coatings and RF discharges were used to modify anode contaminants from field-threshold LiF ion sources. RF discharges and cryogenic-cathode cooling were used to modify contaminants on stainless or titanium cathodes. An inductively-coupled technique enabled heating of the anode to 600 °C in 10 seconds. Temperatures of 200 - 400 °C were typically maintained for up to 30 minutes. 5000 Å thick Au and Ta coatings underneath LiF lithium ion source films were used to suppress desorption from the substrate oxide which was difficult to clean in-situ. Thicker coatings (3 µm) on stainless substrates with improved surface finish (< 0.2 µm RMS) give improved coverage, and have recently shown further performance improvements. These films also demonstrated that thermal desorption of contaminants was important in ion diodes (as in electron diodes) and that the LiF film morphology allowed desorption from the underlying substrate into the AK gap. The discharge protocol used Ar and Ar/O<sub>2</sub> at low pressure to maximize contaminant removal rate, in a configuration where the anode was the RF electrode for direct sputtering of the anode and cathode electrodes. Pumpout delays for the removal of the discharge gas prior to accelerator firing were 30 - 120 seconds.

The combination of RF discharge cleaning, Au or Ta coatings and the moderate heating protocol above allowed improved lithium beam production and contamination beam reduction. Fig. 3 shows that an overall factor of 4 improvement in lithium current density has been possible in two different ion diode field profile configurations using these techniques. Increased lithium current density is coupled with larger voltage and near anode electric field, and reduced anode plasma. Proton contamination was reduced by a factor of 5 to 10. Control of C beam contamination was still an issue. Anode VUV spectroscopy showed a factor of 3 to 10 reduction in C and O contaminant ion line emission [17,18,89]. This is the first experiment where an increase in the lithium current density was observed with cleaning, perhaps because of the field-threshold nature of the source [18]. Longer discharge cleaning was required to affect cathode plasma than to improve lithium beam purity, and this was related [18] to the differences in flux required to clean LiF [64], compared to stainless [61,62].

Cryogenically-cooled cathodes [90] on SABRE ( $\approx 120$  °K) showed improvement in applied-B diode behavior (lower electron loss, higher lithium current) resulting from cathode plasma modification [18]. Possible explanations for this effect are that cathode plasma generation is delayed or reduced. Cryogenically cooled surfaces have more stable adsorbate layers than surfaces at room temperature [91]. Cryogenically-cooled electrodes have shown an increase in the breakdown strength of DC gaps and in the delay to breakdown, depending on which electrode has been cooled [1,91].

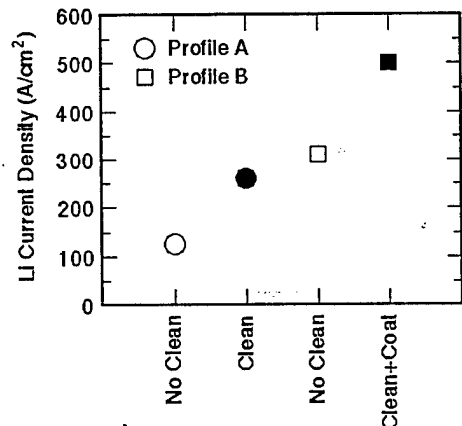


Fig. 3. SABRE lithium current density vs. condition [18].

A further improvement in discharge cleaning [18] was made in subsequent extraction diode experiments on the 30 TW PBFA-X accelerator. Base pressures were improved by a factor of 20, and the pumpout delay was reduced a factor of 4 for a net reduction in re-contamination flux by a factor of 20 - 200. This reduction was combined with a factor of more than 10 increase in the sputtering flux up to  $4e19$  cm<sup>-2</sup> (Ar/O<sub>2</sub>) to produce much larger impedance increase than was observed previously on SABRE. Power, energy and impedance were increased by factors of 27%, 71%, and 150-400% for a 2.5 cm gap extraction ion diode. The pulselength was increased by 20 - 30 ns. Lithium beam power was increased by a factor of 2 at a 2cm AK gap. These experiments produced a record amount of Li in an extraction diode (4 TW) at the highest ion energy at peak ion power. Much of the increase in delivered energy, power, and diode impedance are believed to result from cathode plasma

control, while the improvement in lithium intensity has been correlated with a reduction in contaminant ions.

Recent SABRE ion diode experiments have clearly shown the dominant effects of cathode and anode plasma on diode voltage history and impedance collapse. Fig. 4 gives lithium beam energy (AK gap voltage) histories from 4 different conditions, each the average of 2 to 5 identical shots. Error bars are noted, with the number of shots averaged in parenthesis. The shortest pulse occurred for a new cathode, where not even machining oils were removed prior to firing (open circles, NK/NC). Discharge cleaning (Ar/O<sub>2</sub>) a new cathode significantly increased the pulsedwidth (filled circles, NK/C). About 6 pulses on the new cathode (without cleaning), also appeared to condition cathode plasma, and this occurred despite the fact that the cathode was exposed to air in between each shot (open squares, CK/NC). Several effects could have contributed to this, including cleaning, and smoothing and cleaning of the surface by redeposition of vacuum melted metals during the arc phase after the diode shorts, as noted by SEM and x-ray microprobe analysis. The combination of discharge cleaning and conditioned cathodes (filled squares, CK/C) had a further 10 ns effect on pulsedwidth. Most of the improvement in pulsedwidth resulted from changes to the cathode suggesting that cathode plasma dominates the pulsedwidth although there is a strong coupling between ion current, impedance collapse and anode and cathode plasma motion. This level of plasma mitigation is entry level for the production of high-brightness lithium ion beams.

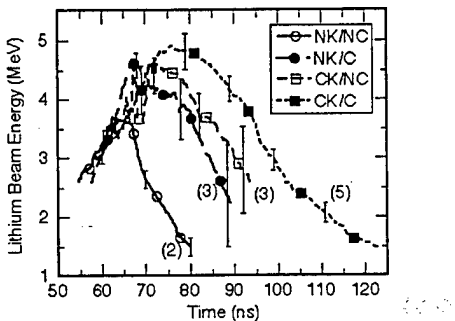


Fig. 4. SABRE voltage history versus condition (NK - new cathode, CK - conditioned cathode, NC - no cleaning, C - cleaning)

The XPS and TPD results described in Sect. 3 may help explain the improvement in performance above, as a reduction in anode and cathode contaminants available for desorption, a reduction in the resulting neutrals desorbed and therefore the plasma density, and/or a reduction in the effective mass of the plasma and its expansion velocity. Cleaning raises the breakdown voltages by control of contamination, and therefore delays cathode turn-on till later in the voltage rise [49,50,52]. Pure, thick oxide layers as are created by Ar/O<sub>2</sub> discharges [65,67] are known to lower electron field emission [65, 92], although large effects on breakdown strength from thick oxide layers were not expected [92]. Differences in cathode spot electrode damage, erosion rates, and mobility have been correlated with the presence of contaminated surfaces [71, 93], and could also be relevant.

Stark shifts of the LiI, 2s-2p 6708 Å transition have been used to measure the electric field as a function of space and time, for 16 lines of sight in the SABRE extraction diode

AK gap [94]. This technique is sensitive to of order 3e13 cm<sup>-3</sup> electron densities. Discharge cleaning increases the amplitude and pulsedwidth of the electric field and reduces the rate of the field collapse in a 1 mm chord centered on and parallel to the anode face. In shots without cleaning, E is observed to decrease more rapidly towards zero suggesting plasma formation in the line of sight. Spectroscopic measurements also show that large changes in the cathode plasma density are possible. Detailed analysis of this data is ongoing for insights into diode physics.

A technique for reaching low diode region base pressures on large volume pulsed-power systems has recently been developed [90]. This method utilizes a differentially-pumped load configuration with large areas of liquid-N<sub>2</sub> and He cryogenically-cooled gettering surfaces. Base pressures of 5e-8 Torr have been obtained on SABRE in a few hours, reduced from 2e-6 Torr. This increases the monolayer collision times up to 10 - 100 seconds for all contaminants with A<20, allowing preservation of an electrode state with < 1 ml adsorbed contaminants following cleaning. Low base pressures are an important piece of an integrated cleaning and conditioning solution.

In summary, cleaning techniques on ion diodes have produced higher diode impedance, higher energy and power entering the diode, higher lithium purity, current density, and energy, lower electron loss, and reduced proton contamination of the beam, and improved beam profile control through control of both anode and cathode plasma. Control of carbon contamination still requires understanding and development. Cleaning is an enabling technology for the generation of high-power ion beams.

#### 4.4 Microwave Devices/RF Cavities

The high current density available from pulsed-power driven electron diodes offers the potential for extracting high-peak power microwaves from electrons traveling in slow- and fast-wave structures. Applications include compact, high energy ( $\geq 1$  kJ) pulsed sources of high-power microwaves to disable military aircraft radar. Higher-power microwave (HPM) systems are also desired to generate higher-accelerating gradients for particle accelerators [95]. A plethora of device configurations exist, but all pulsed-power driven devices appear to be plagued by constant energy output where shorter pulses are obtained at higher output power [96]. Although cold-cathode electron sources are often used, pulse-shortening does not appear to result from AK gap closure in the electron beam diode but from phenomenon in the beam modulation or power extracting structures. The problems of pulse shortening in high-power microwave tubes have been thoroughly reviewed in [96].

Operation of low power (1 - 100 MW) DC tubes require low outgassing materials, low base pressures (< 1e-8 Torr), and careful consideration of electrode material, current contact material, and vacuum seal selection, brazing techniques, pre-assembly cleaning, handling, and surface coatings [95,97]. Many days of pre-assembly and in-situ heat treatments at 350 - 800 °C [95,97] are required for removal of contaminants that limit electric field strengths. Beam-wall interactions must be minimized. Finally, multiple pulse conditioning at gradually increasing power for several days is also necessary to achieve full DC operational levels [95,97]. The HPM experiments where pulse-shortening is observed are typically done under the same technical vacuum conditions that have been discussed previously with no conditioning. These

conditions are known to cause electric field limitations resulting from premature plasma formation, breakdown, loading effects and others [34], that are caused by stimulated desorption, enhanced field emission, secondary electron emission and multipactoring effects.

TiO<sub>2</sub> surface coatings produced by Ar/O<sub>2</sub> ion beams extended the microwave pulselength by a factor of 3 in a slow-wave structure at powers of 40 - 80 MW by control of electron emission and plasma formation [55,98]. Up to 100 conditioning pulses were required to attain the benefit of coating on pulselength. Cr coatings which have reduced secondary electron emission coefficient have shown a further increase in the pulselength. The correlation between beam disruption, electron emission and microwave pulse termination was suggestive of plasma formation on the slow-wave-structure.

The pulselength of a Reltron tube was extended by improved vacuums and multiple pulse conditioning [99]. Pressures above 2e-4 Torr led to rapid degradation of the output power. Material selection and beam-grid interactions were also important factors in pulse-shortening in this tube. The best performance was obtained with rep-rates of more than 10 Hz where it is thought that the surfaces become hot enough to prevent gettering of contaminants, and the high power fluxes produce polymerized coatings with reduced field emission and secondary electron emission [34]. Field strengths of more than 1.5e7 V/m were correlated with reduced microwave output pulselengths, and fields of 3 to 4.5e7 V/m were required in the output cavity for some frequencies. Peak powers of 600 MW have been attained at 1 Ghz using these techniques.

#### 4.5 Other Applications

An overnight argon discharge cleaning improved a plasma opening switch risetime by about 20%, which was believed due to lowered plasma inventory in the switch region [100].

Flashover is thought related to an avalanche in a gas layer produced by stimulated desorption [36,37]. If so, control of the surface gas load or a modification of the secondary electron emission coefficient might raise the flashover threshold field. Atmospheric discharges increased the flashover strength of straight insulators of particular materials, but only to a level near that achieved with 45° insulators. Discharges did not raise the flashover voltage for insulators near the optimum angle [101]. Discharges [102], cryogenically cooled cathodes [91,103], and surface coatings [102-105] have all shown some modification of insulator flashover strength for straight insulators. The improvements do not appear to be as large as those achieved simply by going to 45° insulators for short pulses. Further study of these issues is warranted.

Other applications expected to improve with contamination control include wire array z-pinchers, and immersed diodes for radiography.

### 5. CONCLUSIONS and RECOMMENDATIONS

Possibilities abound for future work in this area. Cleaning techniques show considerable promise for the control of anode and cathode plasma effects in short-pulse, high-energy-density experiments.

(i) Plasmas do limit performance in pulsed-power devices, but with cleaning we do not have to accept all of these limitations. Control of contamination and desorption to the

sub-monolayer level that has resulted in large performance improvements in other fields is still to be demonstrated in a pulsed-power environment. The limits for improved performance through cleaning techniques therefore may not have been reached. We should examine the further combination of these techniques to produce an integrated surface and bulk contaminant and particulate control protocol to see what improvements are possible.

(ii) High spatial- and time-resolved spectroscopic studies of anode and cathode plasma behavior in pulsed-power devices are required to move beyond the early "kitchen-physics" stage of some of the experiments described above. A fundamental understanding of the microphysics of formation, expansion, and modification of these plasmas by cleaning is still required.

(iii) Real pulsed-power systems have non-ideal boundaries with desorption from gassy oxide surfaces and plasma formation, which interact with and subsequently modify the particle and field dynamics. We need to move beyond PIC codes to new PIC-Fluid hybrid architectures and develop codes with "smart-boundaries" and neutral desorption and ionization physics [33,45,46]. Experiments should try to modify their non-idealities by mitigation of plasmas to move behavior towards those of the more ideal simulations.

(iv) The expertise of other communities in these cleaning areas should be utilized: surface scientists, magnetic fusion, high-energy-physics accelerators, microelectronics, DC microwave-tube designers, and others. Surface science techniques such as AES, XPS, SIMS, SEM, and TPD [25,39,40] need to be applied to develop a microscopic physics understanding of electrode state before and after cleaning and conditioning. The effects of cleaning should also be studied in small scale DC and pulsed experiments. These efforts are required to push design limits for future larger, very expensive systems.

An extensive understanding of these issues will be required for some extremely challenging pulsed-power missions such as Z [70], X-1, and IVA radiography. These devices will raise electric fields at surfaces to 2e8 - 1e10 V/m with microscopic enhancement, at electrode power densities sufficient to reach temperatures beyond melt in 2 to 50 ns.

### ACKNOWLEDGMENTS

The technical contributions of D. J. Johnson, W. E. Fowler, P. R. Menge, and D. R. Wenger to this work are gratefully acknowledged. We thank D. L. Cook, J. P. Quintenz, and T. A. Mehlhorn for continuous support and encouragement. Sandia is a multiprogram laboratory operated by the Sandia Corporation, a Lockheed Martin Company, for the United States Department of Energy under Contract DE-AC04-94AL85000.

### REFERENCES

- APL -Appl. Phys. Lett.
- BAPS - Bull. Amer. Phys. Soc.
- BPP - Beitr. Plasma Phys.
- JAP - J. Appl. Phys.
- Jpn. JAP - Japanese J. Appl. Phys.
- JVSTA - J. Vac. Sci. Tech. A
- NIM - Nucl. Instrum. Meth.
- PRL - Phys. Rev. Lett.
- SPTP - Sov. Phys. Tech. Phys.
- STPL - Sov. Tech. Phys. Lett.
- TEI - IEEE Trans. Electrical Insulation

TPS - IEEE Trans. Plasma Science  
 nth BEAMS - Proc. nth Int. Conf. on High Power Particle  
 Beams  
 nth PPC - Proc. nth Int. Pulsed Power Conference

[1] G.A. Mesyats, D.I. Proskurovsky, *Pulsed Electrical Discharge in Vacuum*, (Springer-Verlag, 1988).  
 [2] R.V. Latham, Ed., *High Voltage Vacuum Insulation*, (Academic Press, 1995).  
 [3] J.M. Lafferty, Ed., *Vacuum Arcs: Theory and Application*, (Wiley, 1980).  
 [4] R.J. Noer, *Appl. Phys. A*, 28, 1(1982).  
 [5] R.K. Parker, et al., *JAP*, 45, 2463(1974).  
 [6] D.W. Swain, et al., *JAP*, 46, 4604(1975);  
*JAP*, 48, 118(1977); *JAP*, 48, 1085(1977).  
 [7] A.E. Blaugrund, et al., *Phys. Fluids*, 20, 1185(1977).  
 [8] T.W.L. Sanford, et al., *JAP*, 66, 10(1989).  
 [9] M.E. Cuneo, Ph.D. Thesis, U.Mich., 1989.  
 M.E. Cuneo, et al., *TPS*, 15, 375(1987).  
 [10] D.L. Hinshelwood, *TPS*, 11, 188(1983);  
*Ph. D. Thesis*, MIT, 1982.  
 [11] R.B. Baksht, et al., *STPL*, 3, 243(1977).  
 [12] A. Anders et al., *TPS*, 20, 466(1992).  
 [13] D.J. Johnson, et al., *JAP*, 52, 1681(1981); 57, 794(1985).  
 [14] R.W. Stinnett, et al., *TPS*, 11, 216(1983); *TEI*, 20, 807(1985).  
 [15] Y. Maron, *TPS*, 15, 571(1987).  
 [16] R.B. Baksht, et al., *SPTP*, 18, 94(1973).  
 [17] M.E. Cuneo, et al., 10th PPC, Albuq., 640(1995).  
 [18] M.E. Cuneo, et al., *TPS*, 25, 229(1997).  
 [19] Ph. Bernard, et al., *NIM*, 190, 257(1981).  
 [20] H.F. Dylla, *JVSTA*, 1276(1988).  
 [21] H.F. Dylla, *J.Nuc. Mater.*, 93&94, 61(1980).  
 [22] P.A. Redhead, *The Physical Basis of Ultrahigh Vacuum*, (Chapman and Hall, 1968).  
 [23] S. Dushman, J.M. Lafferty, Eds., *Scientific Foundations of Vacuum Technique*, (Wiley, 1962).  
 [24] D. Hayward, B. Trapnell, *Chemisorption*, (Butterworths, 1964).  
 [25] R.I. Masel, *Principles of Adsorption and Reaction on Solid Surfaces*, (Wiley, 1996).  
 [26] R.J. Elsey, *Vacuum*, 25, 299(1975).  
 [27] C. Hayashi, *Trans. 4th AVS Vac. Symp.*, 13(1957).  
 [28] B.B. Dayton, *Trans. 4th AVS Vac. Symp.*, 42(1957).  
 [29] M. Moraw, *Vacuum*, 36, 523(1986).  
 [30] D. Menzel, ch. 4 in *Interactions on Metal Surfaces*, R. Gomer Ed., (Springer Verlag, 1975).  
 [31] J.P. VanDevender, et al., *APL*, 38, 229(1981).  
 [32] W.A. Stygar, et al., 11th PPC, Baltimore, (1997); prvt. comm.  
 [33] R.A. Vesey, et al., to be published *Phys. Plasmas*.  
 [34] J. Halbritter, *JAP*, 53, 6475(1982); *TEI*, 18, 253(1983);  
*TEI*, 20, 671(1985); *Appl. Phys. A*, 39, 49(1986).  
 [35] A.B. Filuk, et al., *PRL*, 77, 3557(1996).  
 [36] R. Anderson, J. Brainard, *JAP*, 51, 1414(1990).  
 [37] E.W. Grey, *JAP*, 58, 132(1985).  
 [38] H. Padamsee, Ch. 12 in Ref. 2.  
 [39] P.A. Redhead, *Vacuum*, 12, 203(1962).  
 [40] G. Carter, *Vacuum*, 12, 245(1962).  
 [41] E. Hantzsche, et al., *J. Phys. D*, 9, 139(1976).  
 [42] E. Hantzsche, et al., *BPP*, 19, 59(1979).  
 [43] R.A. Langley, *J. Nuc. Mater.*, 128, 622(1984).  
 [44] A.A. Avdienko, M.D. Malev, *Vacuum*, 27, 643(1977).  
 [45] D.R. Welch, et al., *Phys. Plasmas*, 3, 2113(1996).  
 [46] T. D. Pointon, et al., *Proc. Laser Inter. and Related Plasma Phen.*, to be pub. (1997).  
 [47] B. Juttner, *NIM*, A268, 390(1988).  
 [48] P. Niedermann, et al., *JAP*, 59, 892(1986).  
 [49] P. N. Chistyakov, et al., *SPTP*, 14, 807(1969); *SPTP*, 17, 646(1972).  
 [50] A.S. Pokrovskaya-Soboleva, et al., *SPTP*, 16, 1876(1972).  
 [51] I. D. Chalmers, et al., *Vacuum*, 32, 145(1982).  
 [52] M.D. Malev, D.C. Weisser, *TEI*, 24, 1019(1989).  
 [53] L. Jedynak, *JAP*, 35, 1727(1964)

[54] P.C. Bolin, J.G. Trump, 3rd ISDEIV, Paris, 50(1968).  
 [55] C.S. Mayberry, et al., *JAP*, 76, 4448(1994).  
 [56] A.P. Solodovnikov, Y.M. Khrnyi, *SPTP*, 18, 543(1973);  
*ibid.*, 19, 1122(1974).  
 [57] A. V. Batrakov, et al., 11th PPC, Baltimore, (1997).  
 [58] R.V. Latham, N.S. Xu, *Vacuum*, 42, 1173(1991).  
 [59] Ch. Renner, *TEI*, 24, 911(1989).  
 [60] M.H. Achard, et al., *Vacuum*, 29, 53(1978).  
 [61] A.G. Mattewson, et al., *Vacuum*, 24, 505(1974).  
 [62] H.C. Hsueh, et al., *JVSTA*, 3, 518(1985).  
 [63] J. Winter, *J. Nuc. Mater.*, 161, 265(1989).  
 [64] P.R. Menge, M.E. Cuneo, *TPS*, 25, 252(1997).  
 [65] R.S. Calder, et al., *TEI*, 25, 363(1990).  
 [66] R.S. Calder, et al., *NIM*, B13, 631(1986).  
 [67] B. Garke, et al., *Vacuum*, 47, 383(1996).  
 [68] M.S. DiCapua, et al., *vol. 3713(1979)*.  
 M.S. DiCapua, *TPS*, 11, 205(1983).  
 [69] M. E. Cuneo, et al., 10th BEAMS, San Diego, 399(1994).  
 [70] R. B. Spielmann, et al., 10th PPC, Albuq. 396(1995); prvt. comm.  
 [71] B. Juttner, Ch. 15 in Ref. 2.  
 [72] J.G. Kelley, et al., *JAP*, 46, 4726(1975).  
 [73] D.J. Johnson, *APL*, 32, 614(1978).  
 [74] R.D. Genuario, V.L. Bailey, *APL*, 33, 694(1978).  
 [75] M. D. Coleman, B. R. Kusse, *TPS*, 13, 149(1985).  
 [76] J.J. Coogan, 8th PPC, San Diego, 559(1991).  
 [77] J. R. Goyer, et al., *TPS*, 25, 176(1997).  
 [78] J. Rintimaki, et al., *BAPS*, 42, 2025(1997).  
 [79] M.P. Desjarlais, *Phys. Fluids B*, 1, 1709(1989).  
 [80] T.A. Mehlhorn, *TPS*, 25, 1336(1997).  
 [81] P.L. Dreike, G.C. Tisone, *JAP*, 59, 371(1986).  
 [82] J.J. Moschella, et al., *JAP*, 70, 3418(1991).  
 [83] G.C. Tisone, et al., 9th BEAMS, Wash., DC, 800(1992).  
 [84] A.B. Filuk, et al., *ibid.*, 794(1992).  
 [85] K.W. Bieg, et al., *JVSTA*, 3, 1234(1985); *ibid.*, 4, 772(1986).  
 [86] E.J.T. Burns, et al., *JAP*, 63, 11(1988).  
 [87] C. Struckmann, B. Kusse, *JAP*, 74, 3658(1993).  
 [88] Y. Hashimoto, et al., *Jpn. JAP*, 32, 4838(1993); *Jpn. JAP*, 33, 5094(1994).  
 [89] T.J. Nash, et al., *RSI*, 64, 2493(1993); A.B. Filuk, et al., 10th BEAMS, San Diego, 414(1994).  
 [90] D.L. Hanson, et al., *JAP*, 70, 2926(1991); *BAPS*, 42, 2025, (1997).  
 [91] B. Mazurek, Ch. 14, Ref. 2; B. Mazurek, et al., *TEI*, 24, 933(1989).  
 [92] R.V. Latham, et al., *TEI*, 24, 897 (1989).  
 [93] J. Achtert, et al., *BPP*, 17, 419(1977).  
 [94] J.E. Bailey, et al., *PRL*, 74, 1771(1995); *Lasers and Pärt. Beams*, 14, 543(1996).  
 [95] G. Caryotakis, *TPS*, 22, 683(1994).  
 [96] J. Benford, G. Benford, *TPS*, 25, 311(1997).  
 [97] G. Dammertz, et al., *Vacuum*, 46, 785(1995).  
 [98] C. Grabowski, et al., *Proc. SPIE* 2843, 251(1996).  
 [99] R.B. Miller, *Proc. SPIE* 2843, 2(1996).  
 [100] M.E. Savage, et al., 10th BEAMS, San Diego, 41(1994); prvt. comm.  
 [101] I. Smith, Pulse Sciences, Inc., prvt. comm.  
 [102] H.C. Miller, *TEI*, 24, 765(1989); also Ch. 8, Ref. 2.  
 [103] T.S. Sudharshan, J.D. Cross, *TPS*, 11, 32(1976).  
 [104] G.L. Jackson, et al., *TEI*, 18, 310(1983).  
 [105] L.L. Hatfield, et al., *TEI*, 24, 985(1989).

M98005897



Report Number (14) SAND-98-1396C  
CONF-980818--

Publ. Date (11) 1998

Sponsor Code (18) DOE/DP, XF

UC Category (19) UC-700, DOE/ER

ph

DTIC QUALITY INSPECTOR 5

19980720 058

DOE